Bonding nature of $LiCoO_2$ by topological analysis of electron density from X-ray diffraction.

Eiji NISHIBORI[a,b*], Takayuki SHIBATA[a], Wataru KOBAYASHI[a], Yutaka MORITOMO[a,b]

[a]*Faculty of Pure and Applied Science, University of Tsukuba, Tsukuba 305-8571, Japan*

[b]*Center for Integrated Research in Fundamental Science and Engineering (CiRfSE), Univ. of Tsukuba, Tsukuba 305-8571, Japan*

Corresponding author

Eiji NISHIBORI

E-mail :nishibori.eiji.ga@u.tsukuba.ac.jp

Tel : +81-29-853-6118

ABSTRACT

Electron density distributions of $LiCoO_2$ have been determined by Maximum Entropy method (MEM) and multipole modeling from synchrotron x-ray powder diffraction data. The localization of Co-3*d* electrons was clearly visualized in the deformation MEM density. An electron density by multipole modeling was investigated by the Bader's topological analysis to reveal bonding characteristics and interactions between the constituted atoms.

Keywords : Quantitative evaluation of bonding nature, electron density, topological analysis, synchrotron radiation X-ray diffraction.

1. Introduction

A lithium cobalt dioxide, $LiCoO_2$, is widely used in the positive electrodes of lithium-ion batteries (LIBs). [1] The crystal structure with $R\bar{3}m$ space group consists of layers of lithium located between slabs of CoO_2 octahedra. [2] Electron distribution of $LiCoO_2$ determines the electrochemical properties and functions. Many attempts in both experimental and theoretical researches such as diffraction [3], spectroscopic studies and density functional calculations (DFT) [4] have been performed to reveal the electron distributions. An X-ray electron density study provides three-dimensional charge distributions of materials. The X-ray electron density study of $LiCoO_2$ single crystal had been reported almost ten years ago [3]. They observed electron density overlap between Co and O atoms indicating covalent bonding.

Recent progress of the X-ray electron density study enables us to evaluate the property of materials from observed electron density. The Bader's topological analysis [5] and Hirshfield surface analysis [6] combined with a multipole modeling [7] can estimate interactions between atoms and/or molecules from X-ray electron density. In addition, stable third-generation SR X-ray sources enable us to measure the high quality diffraction data [8, 9]. We have developed a method for determining accurate charge densities using multiple overlaid SR powder data sets [8, 10, 11, 12]. The error of the structure factors determined by the method is less than 1.0%, which is comparable to that of the very accurate *Pendellösung* method [13] which needs a large perfect crystal of well-defined wedge shape and target materials have been extremely limited such as silicon. The MEM charge densities at the bond midpoints of silicon and diamond were almost equal to theoretical values within 0.05 $eÅ^{-3}$. The method was also applied to a thermoelectric binary-skutterudite $CoSb_3$ [10] and a-rhombohedral boron [12].

$LiCoO_2$ is used as a powder form in an actual electronic device. The electron density study from powder diffraction using the present state of the art experimental and analytical technique would provide crucial information for understanding the properties. In this study, we investigated an X-ray electron density of $LiCoO_2$ using the multiple overlaid powder profiles technique [8].

2. Experimental

Polycrystalline sample of $LiCoO_2$ was sealed in a 0.3 mm internal diameter Lindeman glass capillary. SR powder X-ray profiles were measured at the SPring-8 BL44B2 beamline [14]. A large

Debye-Sherrer camera with an imaging plate (IP) detector was used for data collection. The data were collected at 100 K using a N_2 gas flow low temperature device. The wavelength of the incident X-rays was 0.45018 Å by calibration with a NIST CeO_2 standard sample. The high energy X-ray was used for reducing the effect of absorption and extinction. Four powder profiles were measured on the same sample to improve the counting statistics of the reflections. The first powder profile was measured using the normal procedure. The 2θ region was from 0.010° to 74.64° with 0.01° step width, and the exposure time was 6 minutes. The exposure time was the time for the maximum intensity of the 002 reflection to become 80 % of the detection limit for the IP. Second, third, and fourth profiles were measured to improve the counting statistics of the middle and high order reflections from 18.41° to 98.60°, 35.10° to 115.05°, and 55.93° to 136.02° in 2θ. The exposure time of second, third, and fourth profiles were 24, 96, and 192 minutes. The first, second, third and fourth profiles from 4.0° to 71.40°, 19.0° to 81.75°, 35.80° to 90.0°, and 56.3° to 102.40° were used for a structural analysis. The resolution in *d*-spacing corresponds to 0.289 Å.

3. Results and discussion

We have developed Rietveld refinement software for multiple powder profiles [8]. Four powder profiles were analysed with the Rietveld refinement. The fitting result of Rietveld refinements were shown in Fig. 1. The reliability factors based on the weighted profile, R_{wp}, and the Bragg intensities, R_I, were 1.19 and 2.07 %, respectively.

The electron density study by the Maximum Entropy method (MEM) was carried out with the program package ENIGMA [15]. The MEM for a crystallographic Fourier inversion problem is a

powerful tool for the electron density determination from a limited number of structure factors. The high-resolution electron density without truncation effect can be obtained by the MEM. A total of 578 structure factors were extracted from the four powder data sets and these were used in the analysis. The procedures were described in our previous papers [8, 10]. The data resolution of the MEM analysis is better than 0.29 Å in *d*-spacing. The unit cell was divided into 36×36×180 pixels. The reliability factors of MEM analysis, R_{MEM} and *wR*, were 0.73 % and 1.08 %, respectively.

Fig. 2(A) shows a total MEM electron density, ρ_{obs}, of $LiCoO_2$ at 100K for 104 plane. The schematic representation of a plane is shown as inset. Li, Co, and O atoms are located on the plane. The charge densities of Li ions are isolated from the CoO_2 slabs in this figure. There are electron density overlaps between O and Co. The ρ_{obs} is dominated by the core electrons and the effects of chemical bonding are only slightly visible. In order to investigate the bonding nature of the MEM densities in detail, we calculated a deformation density from MEM electron density expressed as $\rho_{def}=\rho_{obs}-\rho_{calc}$.[16] We can recognize deformation of valence electrons in the ρ_{def} .The ρ_{calc} were calculated by MEM using the calculated structure factors from Rietveld refinement. Fig. 2 (B) shows the deformation density for 104 plane. Electrons in Co-3*d* orbitals are clearly recognized as positive and negative charge densities around Co sites. The electron density overlap between Co and O did not found in the deformation density. There were negative charge densities indicating lack of electrons at Co-O bond midpoint.

In order to quantitatively estimate bonding interaction of $LiCoO_2$, the Bader's topological analysis was performed using a multipole modeling electron density. We did a multipole electron

density modeling using program *XD* [17] using the Hansen Coppens formalism[7]. The formalism describes the electron density in the crystal by a superposition of aspherical pseudoatoms modeled by a nucleus-centered multipole expansion

$$\rho_k(\boldsymbol{r}) = P_c\rho(r) + P_v\kappa^3\rho_v(\kappa r) + \kappa'^3\sum_{l=1}^{4} R_l(\kappa' r)\sum_{m=1}^{l} P_{lm\pm}d_{lm\pm}(\boldsymbol{r}/r) \qquad (1)$$

where ρ_c and ρ_v are the free-atom Hartree Fock core and the valence densities, $d_{lm\pm}$ are the real spherical harmonic functions, R_l are the Slater-type radial functions including a factor r^n; κ and κ' are the expansion-contraction parameters, P_v and $P_{lm\pm}$ are the populations. The R_F and Rw_F of multipole modeling were 1.0% and 0.77%, respectively which are much smaller than those of an independent spherical atom model, 3.22% and 2.38%. Fig. 3(A) shows a trajectory of $\nabla\rho(r)$. The space of the electron density distribution is partitioned into regions as the atomic basins. Fig. 3(B) shows atomic basins of Li, Co, and O atoms. The atomic basins of Li, Co, O atoms are also recognized in Fig. 3(A). Li and Co basins contact with O basins indicating bonding interaction.

There are bond critical points (BCPs) between Li and O, and Co and O shown as blue circles in Fig. 3(A). In the Bader's topological analysis, the bonds are classified by the values of Laplacian, $\nabla^2\rho(r)$, at BCPs. The $\nabla^2\rho(r)$ for the covalent bond is negative indicating a concentration of electron density in the internuclear region. The $\nabla^2\rho(r)$ for the closed-shell interaction is positive indicating a deep minimum along the path connecting the nuclei. The $\nabla^2\rho(r)$ at BCPs of Co-O is 12.6 eÅ^{-5}. Large positive Laplacian at Co-O bond indicates closed-shell interaction indicating ionic bond. Laplacian in the typical ionic systems have been reported in the Bader's text book [5]. The Laplacian of bond critical point for LiF and NaCl are 16.94 eÅ^{-5} and 4.83 eÅ^{-5}, respectively. Ionic interaction

of Co-O is close to that of LiF.

In summary, the large positive Laplacian at Co-O bond critical point and a lack of electron Co-O region in the deformation MEM electron density suggests that a slab of CoO_2 octahedra is mainly stabilized by ionic interaction. The localization of Co-3*d* orbital causes an ionic interaction of Co-O. The quality of X-ray data and analytical techniques are improved during past couple of decade by the progress of X-ray source and computational technique. The systematic X-ray electron density studies of batteries materials may show the guideline for synthesis of high-performance materials.

Acknowledgement

This work was supported by G Grant-in-Aid for Challenging Exploratory Research (no. 25600148). We thank Dr. Kato for experimental help at SPing-8 BL44B2. The synchrotron radiation experiments were performed at BL44B2 in SPring-8 with the approval of RIKEN (Proposal No. 20140077).

References

1. K. Mizushima, P.C. Jones, P.J. Wiseman, J.B. Goodenough, *Mat. Res. Bull.* **15**: 783 (1980).

2. H. J. Orman and P. J. Wiseman, *Acta Cryst.* C**40**, 12 (1984).

3. Y. Takahashi, N. Kijima, K. Dokko, M. Nishizawa, I. Uchida, J. Akimoto, *J. Sol. Stat. Chem.* **180**

313 (2007).

4. G. Kresse and J. Furthmuller, *Phys. Rev.* B**54** 11169 (1996).

5. R. W. F. Bader, *Atoms in Molecules: A Quantum Theory.* Oxford University Press (1994).

6. J.J. McKinnon, M.A. Spackman, A.S. Mitchell, *Acta Cryst. B***60**, 627 (2004).

7. N..K. Hansen & P. Coppens, *Acta Cryst.* A**34**, 909 (1978).

8. E. Nishibori, E. Sunaoshi, A. Yoshida, S. Aoyagi, K. Kato, M. Takata, M. Sakata. *Acta Cryst.*, A**63** 43 (2007).

9. N. Bindzus, T. Straasø, N. Wahlberg, J. Becker, L. Bjerg, N. Lock, A. C. Dippel, B. B. Iversen, *Acta Cryst.* A**70**, 39 (2014).

10. A. Ohno, S. Sasaki, E. Nishibori, S. Aoyagi, M. Sakata, B. B. Iversen. *Phys. Rev.* **B76**, 064119 (2007).

11. H. Svendsen, J. Overgaard, R. Busselez, B. Arnaud, P. Rabiller, A. Kurita, E. Nishibori, M. Sakata, M. Takata and B. B. Iversen. *Acta Cryst.* A**66**, 458 (2010).

12. E. Nishibori, H. Hyodo, K. Kimura, M. Takata, *Sol. Stat. Sci.* (2015) inpress.

13. T. Saka, and N. Kato. *Acta Cryst.* A**42,** 469, (1986).

14. K. Kato, R. Hirose, M. Takemoto, S. Ha, J. Kim, M. Higuchi, R. Matsuda, S. Kitagawa, & M. Takata, *AIP Conf. Proc*, **1234**, 875 (2010).

15. H. Tanaka, M. Takata, E. Nishibori, K. Kato, T. Iishi, M. Sakata, *J. Appl. Cryst.* **35**, 282 (2002).

16. E. Nishibori, T. Nakamura, M. Arimoto, S. Aoyagi, H. Ago, M. Miyano, T. Ebisuzaki, M. Sakata. *Acta Cryst.* **D 64**, 237 (2008).

17. A. Volkov, P. Macchi, L. Farrugia, C. Gatti, P. Mallinson, T. Richter, T. Koritzansky, *XD2006. A*

Computer Program Package for Mulitpole Refinement, Topological Analysis of Charge Densities and Evaluation of Intermolecular Energies from Experimental and Theoretical Structure Factors. University at Buffalo, State University of New York, USA; University of Milan, Italy; University of Glasgow, UK; CNRISTM, Milan, Italy; and Middle Tennessee State University, USA. (2006).

Figure Captions

Fig. 1 Fitting results of Rietveld refinement for $LiCoO_2$. The four powder profiles with different X-ray exposure time and 2θ range were shown. Four data were analyzed simultaneously and the scaling between the multiple powder profiles was carried out within the refinement.

Fig. 2. (a) The total electron density for 104 plane determined by the Maximum Entropy Method from powder diffraction data. Contour lines were drawn from 0.0 to 3.0 with 0.3 $eÅ^{-3}$ step width. (b) The MEM deformation density for 104 plane. Contour lines were drawn from -1.0 to 1.0 with 0.2 $eÅ^{-3}$ step width. The density is also represented by a color, indicated by the color bar.

Fig. 3 (A) The trajectory of $\nabla\rho(r)$ for a multipole modeling electron density with bond critical points (blue) and ring critical points (green). (B) Atomic basins of ions for $LiCoO_2$. Different colors are used for each ions: green (Co), blue (O), and yellow (Li).

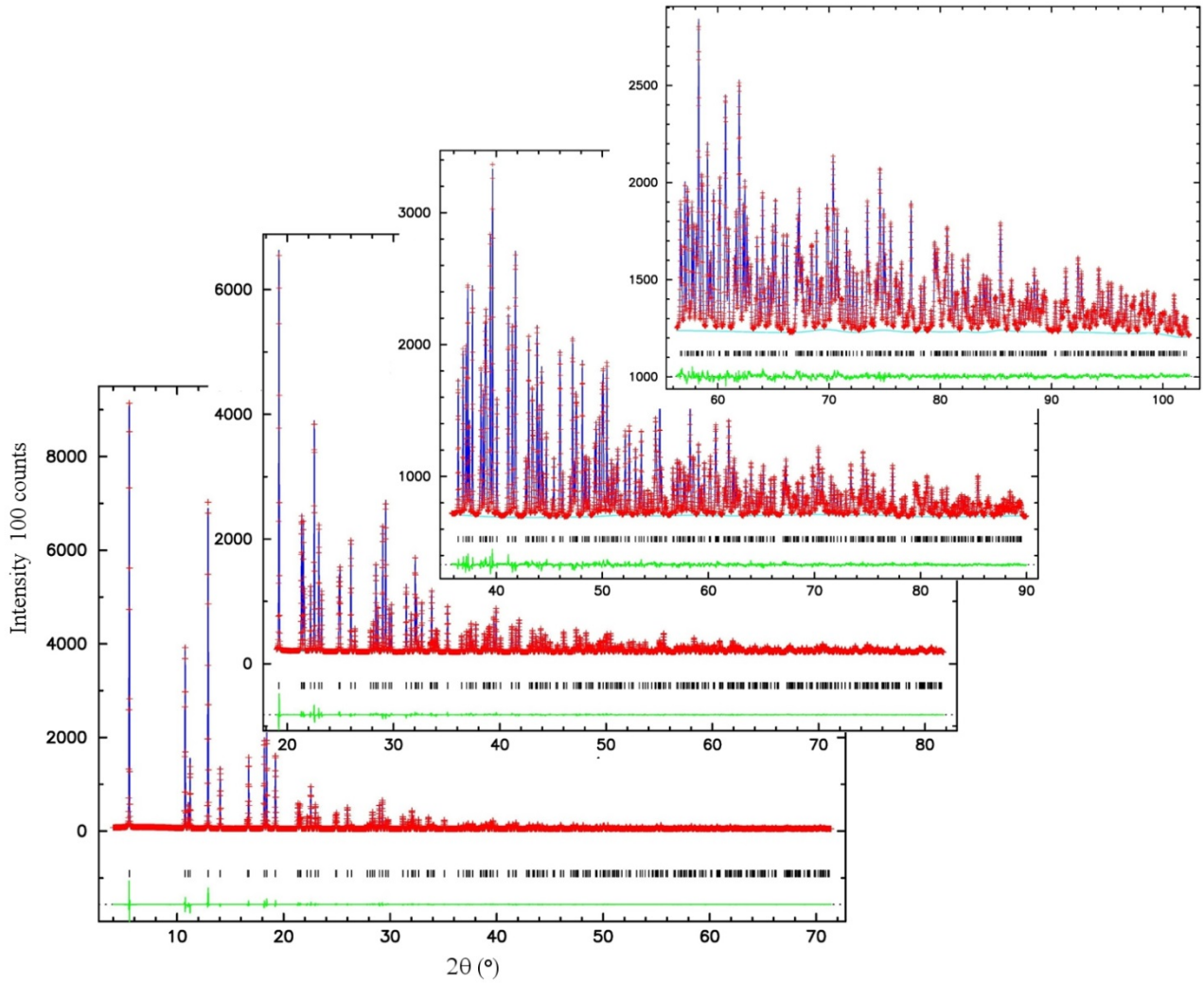

Figure 1

(A) (B)

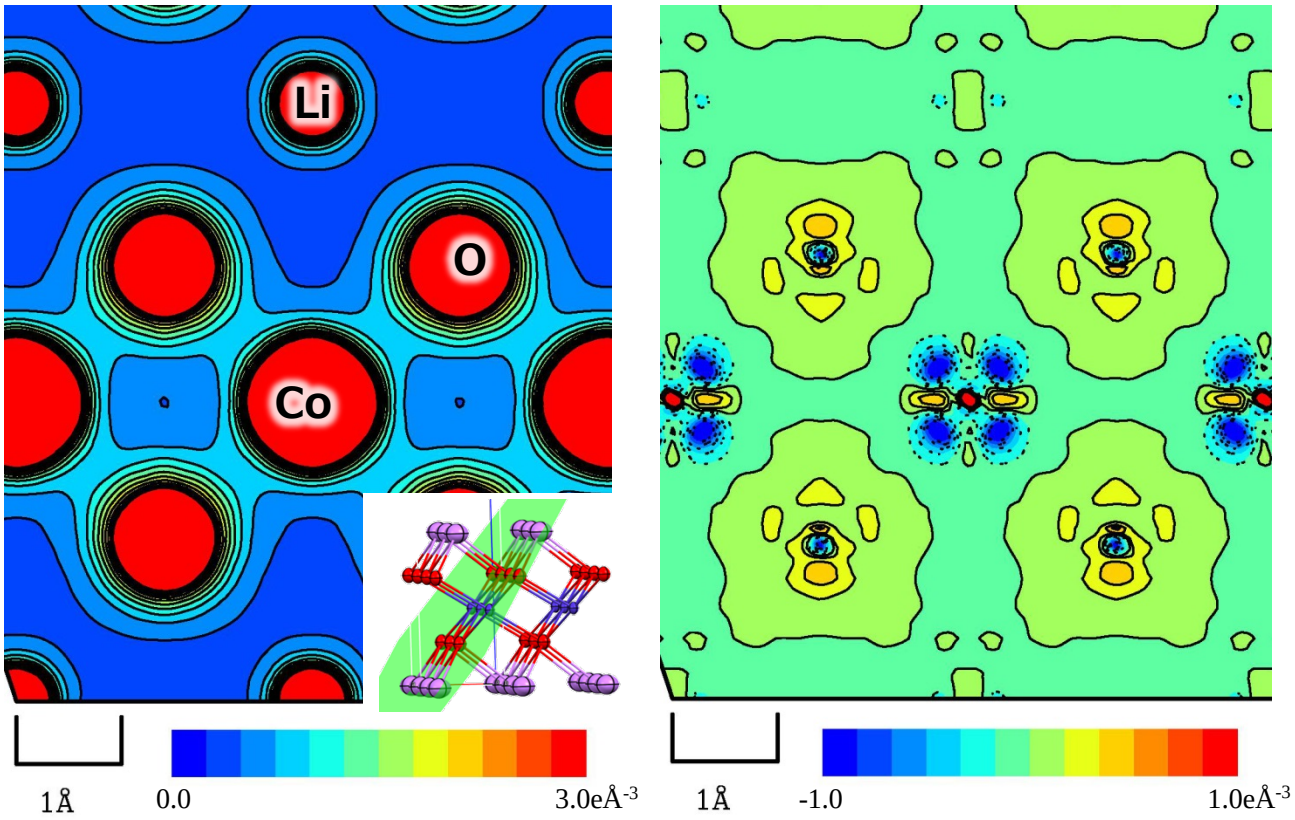

Figure 2

(A)

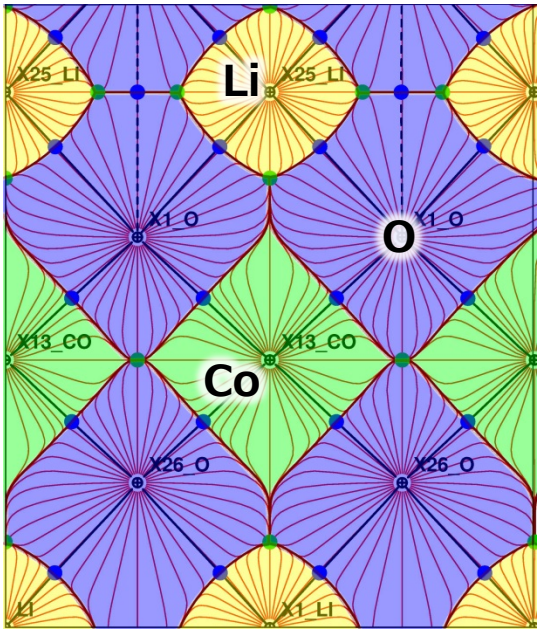
Li
X25_Li
X25_Li
X1_O
O
X1_O
X13_CO
X13_CO
Co
X26_O
X26_O
Li
X1_Li

(B)

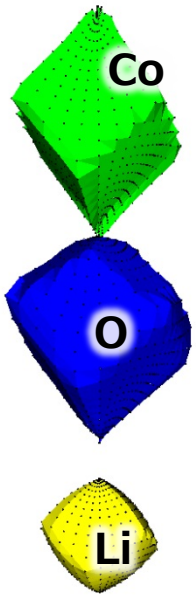
Co
O
Li

Figure 3